EUROPEAN ORGANIZATION FOR NUCLEAR RESEARCH

Proposal to the ISOLDE and Neutron Time-of-Flight Committee

Beta-delayed Neutron Spectroscopy of $^{130-132}$Cd Isotopes with the ISOLDE Decay Station and the VANDLE array

[submission date]

M. Madurga[1], R. Grzywacz[1,2], K. Kolos[1], D. Bardayan[3], M.J.G. Borge[4], N.T. Brewer[2], J.A. Cizewski[5], T. E. Cocolios[6], I. Dillman[7], A. Fijalkowska[8], C.J. Gross[2], K.C. Goetz[1], S.V. Ilyushkin[9], C. Mazzocchi[8], B. Manning[5], K. Miernik[8], D. Miller[7], S.V. Paulauskas[10], W.A. Peters[11], S. Taylor[1], A. Ratkiewicz[4], K. P. Rykaczewski[2] , Y. Xiao[1]

[1]Dept. of Physics and Astronomy, University of Tennessee, Knoxville, Tennessee 37996, USA.
[2]Physics Division, Oak Ridge National Laboratory, Oak Ridge, Tennessee 37830, USA.
[3]Institute for Structure and Nuclear Astrophysics, Department of Physics, University of Notre Dame, Notre Dame, Indiana 46556, USA.
[4]CERN, Geneva, Switzerland
[5]Dept. of Physics and Astronomy, Rutgers University, New Brunswick, NJ 08903 USA.
[6]School of Physics & Astronomy, The University of Manchester, Manchester M13 9PL, UK.
[7]TRIUMF, 4004 Wesbrook Mall, Vancouver, British Columbia V6T 2A3, Canada.
[8]Faculty of Physics, University of Warsaw, PL 00-681 Warsaw, Poland
[9]Department of Physics, Colorado School of Mines, Golden CO 80401.
[10]Department of Physics & Astronomy, Michigan State University, East Lansing, Michigan 48824, USA.
[11]Joint Institute for Heavy-Ion Research, Oak Ridge, Tennessee 37831, USA.

Spokesperson(s): Miguel Madurga Flores (mmadurga@utk.edu)
Robert Grzywacz (rgrzywac@utk.edu)
Local contact: Miguel Madurga Flores

CERN-INTC-2014-040 / INTC-P-412
27/05/2014

Abstract

We propose to use the new ISOLDE decay station and the neutron detector VANDLE to measure the beta-delayed neutron emission of N=82-84 $^{130-132}$Cd isotopes. The large delayed neutron emission probability observed in a previous ISOLDE measurement [M. Hannawald et al., Phys. Rev. **C62**, 054301 (2000)] is indicative of the Gamow-Teller transitions due to the decay of deep core neutrons. Core Gamow-Teller decay has been experimentally proven in the ^{78}Ni region for the N>50 nuclei using the VANDLE array. The spectrocopic measurement of delayed neutron emission along the cadmium isotopic chain will allow us to track the evolution of the single particle states and the shell gap.

Requested shifts: 22 shifts

Introduction

The properties of nuclei in the vicinity of doubly-magic neutron and proton numbers are some of the most sought-after experimental data. The mass, radius, and decay lifetime of spherical shell nuclei are not only important to benchmark theoretical models, but often required ingredients of reactor and stellar nucleosynthesis calculations. In particular, the beta-decay lifetime is connected with nuclear structure through the strength function $S_\beta(E)$:

$$\frac{1}{T_{1/2}} = \sum_{E_i \geq 0}^{E_i \leq Q_\beta} S_\beta(E_i) \times f(Z, Q_\beta - E_i)$$

where $f(Z,Q_\beta-E_i)$ is the Fermi integral. Therefore, the details of the structure of a nucleus play an important role in the beta-decay properties. Our recent work [Mad12] showed that the proper treatment of nuclear shell effects by the model is required in order to achieve agreement between experimental and predicted beta-decay half-lives. Global models used to predict beta-decay lifetimes and decay branching ratios are traditionally either too simplistic [Nak97] or do not incorporate enough details of nuclear structure [Mol97] to produce robust predictions. Great advances in the reliability of the calculations are possible due to the improvement of the "microscopic" foundation of the theory [Mol12, Bor05,Fa13,Zh13] or progress in the development of large scale shell model codes.

We propose to measure the N=82-84, A=130-132 Cadmium isotopes by augmenting the ISOLDE beta-decay station with the recently commissioned neutron detector system called the Versatile Array of Neutron Detectors at Low Energy (VANDLE) [Mat09, Pau13, Pet14]. This detector is able to detect neutrons over a wide range of energies, from 100 keV to 6 MeV, owing to the cutting-edge use of digital electronics. The low-energy threshold achieved by VANDLE is crucial for comprehensive measurements of the beta-decay distribution. This is mainly because, in some cases, a significant amount of the strength lies close to the neutron separation energy resulting in emission of low energy "near-threshold" neutrons. It is also possible that the grand-daughter nuclei to be left in an excited state after neutron emission and the decay energy would be shared between the neutron and gamma rays (Fig. 1). For that reason, it is also essential to combine the neutron detection system with efficient gamma-ray detectors. Finally, for two-neutron emitters, the kinetic energy sharing between two particles can render them slow and unobservable in a system with a high detection threshold.

Until recently, energy resolved beta-delayed neutron studies have been relatively unexplored territory in fission fragments. The notable exceptions are studies on chemically selected Arsenic, Bromine and Iodine [Kra79, Ewa84]. In a breakthrough experiment at Holifield Radioactive Ion Beam Facility (HRIBF) at Oak Ridge National Laboratory (ORNL) almost 30 isotopes were investigated with VANDLE, providing data of very neutron-rich nuclei in the regions between Z=29 and Z=52 [Pau13]. In several cases strong neutron resonance-like structures were observed, an expected feature of pygmy Gamow-Teller resonant beta-decay (see Fig. 2). The discovery of large beta-delayed two-neutron emission probability from ^{86}Ga [Mie13] lends credibility to the theoretical predictions for broad multi-neutron emission processes from heavy precursors. However, the significant discrepancy between the observed two-neutron branching ratio and model predictions provides a strong reason to continue collecting experimental data in order to improve the theoretical models. The HRIBF survey of exotic beta-delayed neutron emission in this region of the nuclear chart is far from complete. Future studies will measure the most remarkable cases of the HRIBF survey nuclei more precisely and explore more exotic nuclei.

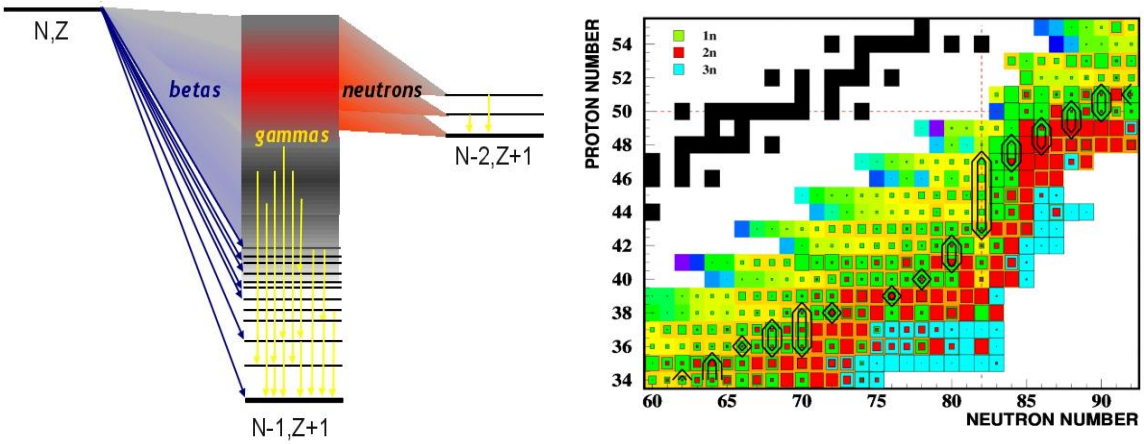

Figure 1. (Left) Schematic of the decay of a neutron-rich nucleus (N,Z) where $Q_\beta > S_n$. The beta decay can populate states above the neutron separation energy (S_n), feeding states in the (N-2,Z+1) daughter. These states de-excite by gamma emission. (Right) Portion of the chart of the nuclides from Sr and beyond Sn isotopes. Color squares indicate isotopes which are candidates for beta-delayed neutron emission [Mol03] . Super-imposed on this figure (black contour) is an example r-process trajectory corresponding to scenarios with neutron density at the freeze-out at 10^{26} cm^{-3}(black), from [Kra07].

Beta-decay of $^{130\text{-}132}$Cd

The region of spherical nuclei around N≥82 and Z≤50 shows a dramatic increase of beta-delayed neutron emission probability (see Fig. 1). Very large Q_β values, in excess of 10 MeV, and a rapid drop of the neutron separation energy, down to about 2 MeV drive the increasing emission probability. Previous measurements of the beta-decay of $^{130\text{-}132}$Cd isotopes have concentrated in the low-energy nuclear structure of $^{130\text{-}131}$In states measuring gamma rays [Dil03,Tap14]. The beta-delayed neutron emission of $^{130\text{-}132}$Cd isotopes has been studied only once before, using the RILIS Laser Ion Source and Mainz neutron Long Counter at ISOLDE [Han00]. Hannawald and collaborators observed a dramatic increase in the neutron emission probability in the isotopic chain, from 3.5% for $^{130\text{-}131}$Cd to 60% in ^{132}Cd. A recent study of the gamma emission following the beta-decay of ^{132}Cd at RIKEN observed a single gamma line in ^{131}In, and no gamma lines in ^{132}In [Tap14]. This could indicate a neutron branching ratio close to 100%, close to shell model predictions, and consistent with Hannawald and collaborators (see below).

Similarly to our ^{84}Ga result [Mad14] we expect to see the neutron emission to be favoured at high energies, indicating the population of narrow B(GT) quasi-resonances. The proximity of the shell closure results in a low level density in the decay daughter, thus one expects the beta decay to proceed via series of "pygmy" resonances, which will reflect single particle nature of the Gamow-Teller transitions (see Fig. 2.) In the case of the nuclei with N>82 and Z<50, the base transitions will be the "spin-flip" $2d_{5/2}\rightarrow 2d_{3/2}$, $1g_{9/2}\rightarrow 1g_{7/2}$, $1h_{11/2}\rightarrow 1h_{9/2}$, "back spin flip" $2d_{3/2}\rightarrow 2d_{5/2}$, $1g_{7/2}\rightarrow 1g_{9/2}$, and "core polarized" $2g_{7/2}\rightarrow 2g_{7/2}$, $2d_{3/2}\rightarrow 2d_{3/2}$, $2d_{5/2}\rightarrow 2d_{5/2}$, $1h_{11/2}\rightarrow 1h_{11/2}$, between single particle neutron and proton orbitals. Figure 4 shows our shell model calculation, ^{100}Sn core, of the Gamow-Teller strength distribution in the beta-decay of 130, 131, and 132 cadmium. The effect of the valence configuration $\pi^{(-2)}+\nu^{(0)\text{-}(2)}$ is approximated by calculating the $\pi^{(2)}+\nu^{(-2)\text{-}(0)}$ space of 132 to 134 Tellurium isotopes. This will qualitatively simulate the effect of pairing and fragmentation due to proton-proton and proton-neutron residual forces. In particular, it is interesting to notice how pairing pushes the Gamow-Teller strength to higher energies in ^{132}Cd. This could possibly explain the large observed increase of the neutron emission probability in the isotopic chain [Han00]. Studying all three N=82-84 isotopes is thus fundamental to track the evolution of the shell gap.

Intriguingly, in the decay of the even-even nucleus ^{132}Cd all neutrons are predicted to be emitted with energies in excess of 2 MeV (Fig. 5).

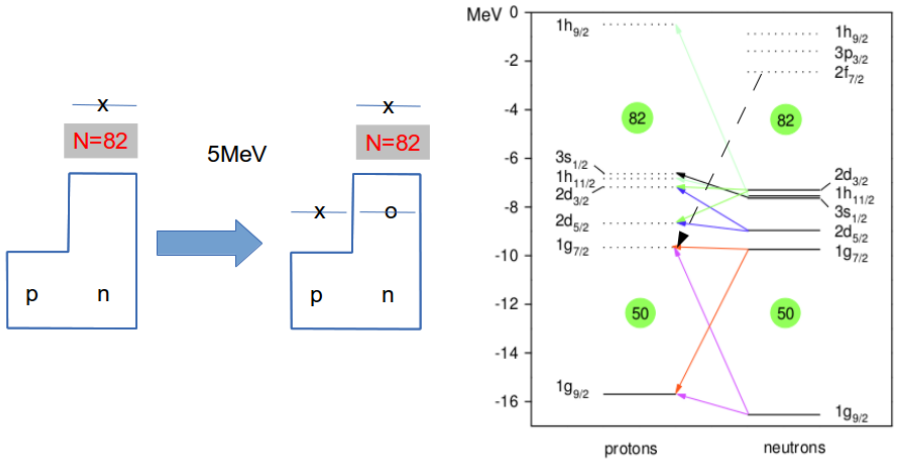

Figure 2: Single particle scheme of the Gamow-Teller beta decay of the nuclei with Z<50 and N>82 close to the doubly magic ^{132}Sn.

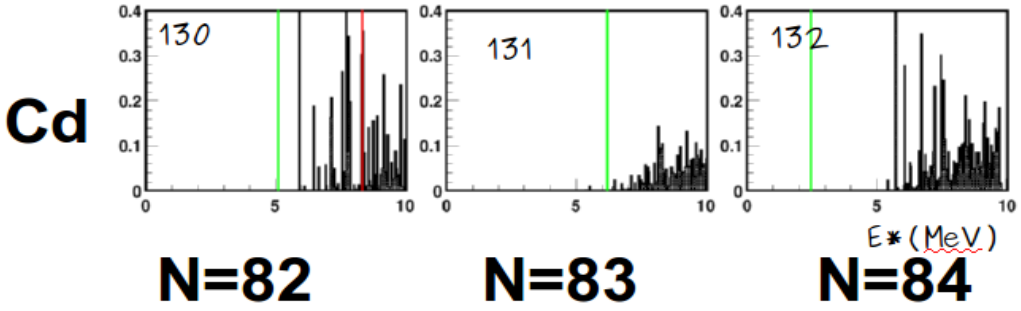

Figure 3: Shell model calculations (this work) of the Gamow-Teller strength in the beta-decay of 130 to 132 Cadmium isotopes. The red line represents the Q_β energy and the green lines the neutron separation energies in 130 to 132 Indium respectively. The Gamow-Teller strength populates unbound states exclusively.

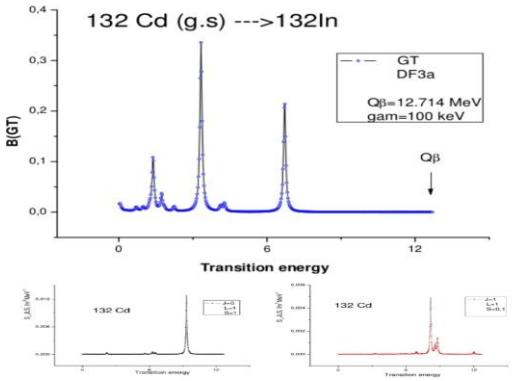

Figure 4: Left: Gamow-Teller strength distribution (top) in the decay of ^{132}Cd predicted by cQRPA calculations by I. Borzov [Mad12]. The two strong peaks are dominated $2d_{3/2} \rightarrow 2d_{5/2}$ single particle transitions (the strongest one) and $1g_{7/2} \rightarrow 1g_{9/2}$. All of the prominent transition will populate neutron unbound states in ^{132}In. First-forbidden strength distributions (bottom).

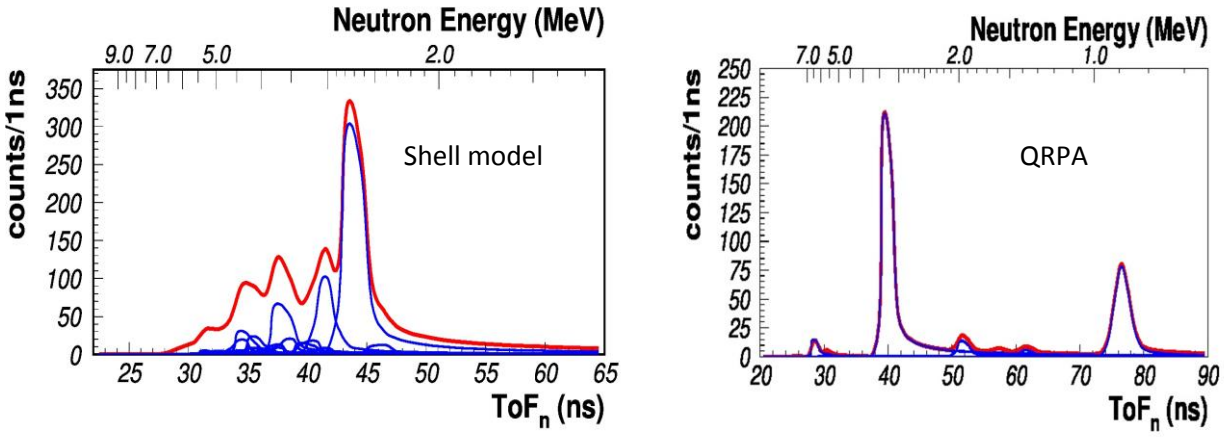

Figure 5: Left: Simulated VANDLE spectrum of the ^{132}Cd decay with 98 cm for time of flight base using the shell-model predictions from Fig. 3. Right: same as in the left, using the decay strength from QRPA calculations in Fig. 4. The peak at 78 ns corresponds to the first forbidden transition and at the 40 ns corresponds to the 7 MeV $1g_{7/2} \rightarrow 1g_{9/2}$ Gamow-Teller resonance. Realistic VANDLE response function is taken into account for both simulations.

Technical Aspects

VANDLE is a modular array of plastic scintillator bars. Plastic scintillators are commonly used for time-of-flight detectors [Sum08] and make a very efficient neutron detector. VANDLE will be placed using a custom-built frame surrounding a partial implementation of the ISOLDE Decay Station [Rap14]. The two top HPGe detectors will be removed for a clear view line for the VANDLE detectors (see Fig. 6). This geometry leaves a total 4% gamma efficiency at 1.3 MeV [Rap14]. The top VANDLE bars will have a 98 cm neutron flight path, housing 26 3x6x120 cm^3 medium VANDLE bars. Another 12 3x3x60 cm^3 small bars are located at a 50 cm flight path, for a 21.8% of 4π acceptance. This allows us to measure the gamma transitions in the daughter nucleus and reconstruct the complete decay scheme including neutrons. The modularity of VANDLE and the use of inexpensive extruded aluminium beams to build the support frame would allow us to quickly reconfigure it to adapt to possible ISOLDE decay station configurations.

The intrinsic efficiency of one VANDLE plastic bar was obtained using the (d,n) calibrated neutron source at Ohio University [Mas98] (see Fig. 7). For the typical energies in beta-delayed neutron emission, 100-4000 keV, the efficiency range is in between 20% to 50%. The angular acceptance of the full array is 23.5% of 4π, giving a total array efficiency of 5-12% in the energy range of interest. For the neutron detection rate estimates we use a conservative 60% beta detection efficiency [Rap14].

The entire system is instrumented with Pixie-16 digital electronics due to its benefits of low energy threshold, simplicity, and stability. We have demonstrated that with a 250 MHz digitization rate we can obtain the sub-nanosecond time resolution required for time-of-flight measurements [Pau14]. A measurement of several beta-delayed neutron precursors was completed in February 2012 at the Low energy Radioactive Ion Beam Spectroscopy Station (LeRIBSS) at HRIBF [Mad14]. The setup consisted of two plastic scintillators (ε~50%, which provided the start signal) and 48 VANDLE bars 51 cm away from the implantation point. Two HPGe clovers were used for high-resolution gamma spectroscopy and beta-gamma-neutron coincidences.

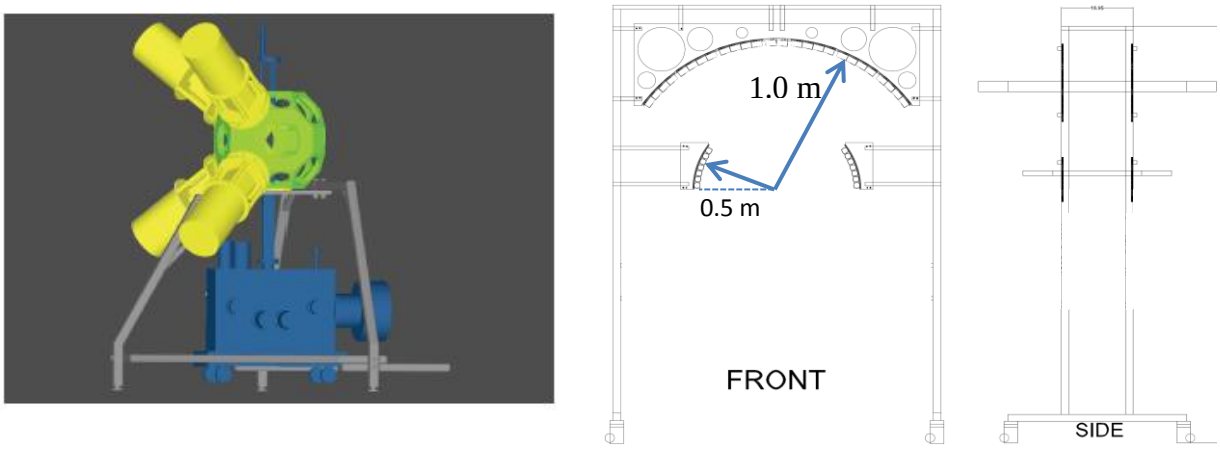

Figure 6: Experimental instruments. Left: proposed configuration of the ISOLDE Decay Station. The two top clovers would be removed to clear the neutron flight path for VANDLE. Right: proposed VANDLE frame. The 4 aluminium legs support VANDLE on top of the existing ISOLDE decay station. It is designed to house 26 medium VANDLE bars (3x6x120 cm^3) at 100 cm and 12 small bars (3x3x60 cm^3) at 50 cm.

In the LeRIBSS data set the intrinsic timing resolution of the VANDLE system digitized in Pixie16 was 700 ps FWHM. The final resolution of 3 ns FWHM was dominated by the timing properties of the long, single photomultiplier, beta scintillators surrounding the implantation point. The timing resolution of the ISOLDE Decay Station beta-tagging system will only be limited to the Pixie16 precision, as each scintillator unit is much smaller than the LeRIBSS system. Because of this we expect to achieve the maximum energy resolution of 6% given by the 3 cm detector thickness over a 100 cm flight path.

Beam Request

Table 1 summarizes the requested beam time. The quality of Cd beams at ISOLDE has been recently shown to be dramatically improved by the use of the RILIS laser ion source, cold quartz line (300º) and a neutron converter [Sto12]. A yield of 1.3 10^4 ions/μC of ^{128}Cd was observed, from which we extrapolate the rates in Table 1. Indium suppression is of the most importance for neutron detection, as it is the only other A=130-132 isobar member with delayed neutron emission. The other large contaminant, caesium, can be minimized using short tape cycles. In the ^{128}Cd test, the ^{128}In component was two orders of magnitude smaller than cadmium. The neutron emission probabilities of $^{130\text{-}131}$In are 1% and 2% respectively, close to the values for Cd isotopes. For these two cases a suppression of one or two orders of magnitude is desired. In the case of the A=132 isobar, the ^{132}In P_n is 10 smaller than that of ^{132}Cd. In this case, it would be possible to take ^{132}In contamination of the same magnitude as the cadmium beam, although a reduction of one order of magnitude or better is desired.

One shift of ^{49}K is asked to do an internal calibration of VANDLE time-of-flight response. The neutron energy spectrum of ^{49}K is well known, having been previously measured at ISOLDE [Per06].

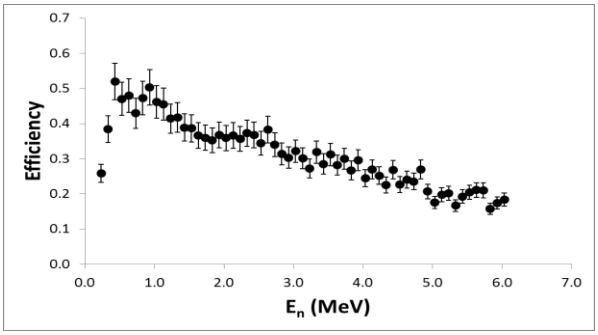

Figure 7: VANDLE detector experimental intrinsic efficiency. The low energy threshold was set at 25 keVee. The total efficiency of the array (100 cm and 70 cm flight paths as shown in Fig. 3) can be obtained by multiplying the intrinsic efficiency times the angular acceptance Ω=41% of 4π.

	P_n (%) [NNDC]	Yield (ion/μC)	VANDLE Eff	Neutrons (1/h)	Shifts**	Target	Source
^{130}Cd	3.5	1000*	0.09	3300	3	UC_x	Ta cavity + n. c. + RILIS
^{131}Cd	3.5	100*	0.09	330	9	UC_x	Ta cavity + n. c. + RILIS
^{132}Cd	60	5*	0.09	280	9	UC_x	Ta cavity + n. c. + RILIS
^{49}K	86	$2.7\ 10^5$	0.09	$21.9x10^6$	1	UC_x	Ta cavity + n. c. + RILIS

*Table 1: Expected neutron rates. The calculated number of neutrons per hour includes 60% beta detection efficiency and 50% transmission/duty cycle efficiency. * The $^{130\text{-}132}Cd$ yields have been extrapolated from the ^{128}Cd test [Sto12].*

Summary of requested shifts:

We request 22 shifts in order to collect at least 10^5 neutrons per Cadmium isotope. Considering the beam rate achievable and their neutron branching ratios, it breaks down to 3 shifts for ^{130}Cd, and 9 shifts for ^{131}Cd and ^{132}Cd each. We ask for 1 shift of ^{49}K for internal calibration.

References:

*[Bor05] I.N. Borzov, Phys. Rev. C**71**, 065801 (2005).*

[Dil03] I.Dillman et al. Phys. Rev. Lett. 91, 162503 (2003).

*[Ewa84] G.T. Ewan et al., Z. Phys. A**318,** 309 (1984).*

*[Fa13] Dong-Liang Fang,B. Alex Brown, and Toshio Suzuki, Phys. Rev. **C88**, 034304 (2013).*

*[Han00] M. Hannawald et al., Phys. Rev. **C62**, 054301 (2000).*

*[Kra79] K.-L. Kratz et al. Nucl. Phys. **A317,** 335(1979).*

*[Kra07] K.-L. Kratz, K. Farouqi and B. Pfeiffer, Prog. in Part. and Nuc. Physics **59** ,147(2007).*

*[Mad12] M. Madurga et al., Phys. Rev. Lett. **109**, 112501 (2012).*

[Mad14] M. Madurga et al., in preparation.

*[Mas98] T.N. Massey et al., Nucl. Science and Engineering **129**, 175 (1998).*

*[Mat09] C. Matei et al., AIP Conf. Proc. **1099**, 790 (2009).*

*[Mie13] K. Miernik et al. Phys. Rev. Lett. **111**, 132502 (2013).*

*[Mol97] P. Möller et al., At. Data Nucl. Data Tab. **66**, 131 (1997).*

*[Mol03]P. Möller, B. Pfeiffer, and K.-L. Kratz, Phys. Rev. C**67**,055802 (2003).*

*[Mol12] P. Möller et al., Phys. Rev. Lett. **108**, 052501 (2012).*

*[Nak97]H. Nakata, T.Tachibana, M.Yamada, Nucl. Phys. **A625**, 521 (1997).*

[NNDC] www.nndc.bnl.gov.

[Rap14] E. Rapisarda. Private Communication.

[Sto12] T. Stora, Private Communication (2012).

*[Sum08] C. S. Sumithrarachchi et al. , Phys. Rev. **C81** , 014302 (2008).*

[Pau13] S.V. Paulauskas, dissertation, University of Tennessee, (2013).

*[Pau14] S.V . Paulauskas et al., Nucl. Instrum Meth. **A737**, 22 (2014).*

[Per06] F. Perrot et al., Phys. Rev. C 74, 014313 (2006)

[Pet14] W.A. Peters et al, in preparation.

[Tap14] J. Taprogge et al., Phys. Rev. Lett. 112, 132501 (2014).

Appendix

DESCRIPTION OF THE PROPOSED EXPERIMENT

The experimental setup comprises: *(name the fixed-ISOLDE installations, as well as flexible elements of the experiment)*

Part of the	Availability	Design and manufacturing
ISOLDE Decay Station	☐ Existing	☐ To be used without any modification
	☒ New	☒ To be modified
VANDLE	☒ Existing	☒ To be used without any modification ☐ To be modified
	☐ New	☐ Standard equipment supplied by a manufacturer ☐ CERN/collaboration responsible for the design and/or manufacturing
[Part 2 experiment/ equipment]	☐ Existing	☐ To be used without any modification ☐ To be modified
	☐ New	☐ Standard equipment supplied by a manufacturer ☐ CERN/collaboration responsible for the design and/or manufacturing
[insert lines if needed]		

HAZARDS GENERATED BY THE EXPERIMENT

(if using fixed installation) Hazards named in the document relevant for the fixed [COLLAPS, CRIS, ISOLTRAP, MINIBALL + only CD, MINIBALL + T-REX, NICOLE, SSP-GLM chamber, SSP-GHM chamber, or WITCH] installation.

Additional hazards:

Hazards			
	[Part 1 of the experiment/equipment]	*[Part 2 of the experiment/equipment]*	*[Part 3 of the experiment/equipment]*
Thermodynamic and fluidic			
Pressure	[pressure][Bar], [volume][l]		
Vacuum			
Temperature	[temperature] [K]		
Heat transfer			
Thermal properties of materials			
Cryogenic fluid	[fluid], [pressure][Bar], [volume][l]		
Electrical and electromagnetic			
Electricity	[voltage] [V], [current][A]		
Static electricity			
Magnetic field	[magnetic field] [T]		
Batteries	☐		
Capacitors	☐		
Ionizing radiation			
Target material	[material]		
Beam particle type (e, p, ions, etc)			

Beam intensity			
Beam energy			
Cooling liquids	[liquid]		
Gases	[gas]		
Calibration sources:	☐		
• Open source	☐		
• Sealed source	☐ [ISO standard]		
• Isotope			
• Activity			
Use of activated material:			
• Description	☐		
• Dose rate on contact and in 10 cm distance	[dose][mSV]		
• Isotope			
• Activity			
Non-ionizing radiation			
Laser			
UV light			
Microwaves (300MHz-30 GHz)			
Radiofrequency (1-300MHz)			
Chemical			
Toxic	[chemical agent], [quantity]		
Harmful	[chemical agent], [quantity]		
CMR (carcinogens, mutagens and substances toxic to reproduction)	[chemical agent], [quantity]		
Corrosive	[chemical agent], [quantity]		
Irritant	[chemical agent], [quantity]		
Flammable	[chemical agent], [quantity]		
Oxidizing	[chemical agent], [quantity]		
Explosiveness	[chemical agent], [quantity]		
Asphyxiant	[chemical agent], [quantity]		
Dangerous for the environment	[chemical agent], [quantity]		
Mechanical			
Physical impact or mechanical energy (moving parts)	[location]		
Mechanical properties (Sharp, rough, slippery)	[location]		
Vibration	[location]		
Vehicles and Means of Transport	[location]		
Noise			
Frequency	[frequency],[Hz]		
Intensity			
Physical			
Confined spaces	[location]		
High workplaces	[location]		
Access to high workplaces	[location]		
Obstructions in passageways	[location]		
Manual handling	[location]		
Poor ergonomics	[location]		

0.1 Hazard identification

3.2 Average electrical power requirements (excluding fixed ISOLDE-installation mentioned above): *(make a rough estimate of the total power consumption of the additional equipment used in the experiment)*

VANDLE requires independent dedicated data acquisition and High Voltage Supply modules. All VANDLE electronics are run through an Uninterrupted Power Supply that typically draws 1000-1200 W.